





Cite this: *Polym. Chem.*, 2022, **13**, 2782

# Sulfur-dipentene polysulfides: from industrial waste to sustainable, low-cost materials†‡

Selena Silvano, <sup>a,b,c</sup> Incoronata Tritto, <sup>\*b</sup> Simona Losio <sup>b</sup> and Laura Boggioni <sup>b</sup>

The synthesis of poly(S-dipentene) with a sulfur content greater than 50 wt% by catalytic inverse vulcanization in the presence of zinc-based accelerators was investigated at 140 °C for the first time. Accelerators reduced the time required for mixing of dipentene and melted sulfur and the best results were obtained with zinc tetrabutyl-bis(phosphorodithioate). Three bio-based dienes, garlic oil (GO), diallyl disulfide (DAS) and myrcene (MYR), were used as crosslinkers in the post-polymerization of poly(S-dipentene). Stable ter-polymers with depressed depolymerization reactions were obtained by adding 10 wt% of MYR, GO or DAS. The ter-polysulfides produced were soft solids with  $T_g$  values between  $-1$  and  $4$  °C. Processable polystyrene–poly(S-dipentene-DAS) blends were prepared with shape persistence, a fundamental requirement to prepare solid objects, and found to be able to remove ferric ions from aqueous solutions for application in wastewater purification. Thus, green polysulfides were obtained, which represent an economical alternative to polysulfides synthesized from enantiomeric limonene.

Received 21st January 2022,  
Accepted 8th April 2022

DOI: 10.1039/d2py00095d

rsc.li/polymers

## Introduction

Nowadays, most of the world's energy comes from fossil fuels; in 2019, the share from fossil resources was still over 84%, half of which was derived from petroleum.<sup>1</sup> The sulfur content in fossil resources affects the value of crude oil. Indeed, sulfur and sulfurated compounds are undesirable for their ability to deactivate some catalysts used in the refining process and because they cause sulfur oxide gas emissions, which lead to acid rain and have a negative impact on the ecosystem.<sup>1,2</sup> For this reason, about 70 million tonnes of elemental sulfur are removed from crude oil each year. Although much of this is used for the production of sulfuric acid, tires and fertilizers, a large volume of sulfur is stored unused in enormous deposits with little economic utility, causing the global issue known as the “excess sulfur problem”.<sup>3</sup> Therefore, in the last few years,

interest in exploring the use of sulfur as a low-cost starting material for the synthesis of sulfur rich-polymers with interesting properties has emerged.<sup>4–6</sup> Polymers with a high sulfur content (>50 wt%) have interesting optical, electrical and antibacterial properties and applications such as Li–S batteries, IR-transparent lenses and metal and oil capture.<sup>7–20</sup>

In 2013, Pyun and co-workers developed a new process, named “inverse vulcanization”, which enabled the direct copolymerization of elemental sulfur with diene comonomers as crosslinkers. In general, inverse vulcanization requires heating sulfur over the floor temperature (159 °C) to allow S–S bond homolysis and provides thiyl radicals which react with diene species to yield a stable material by intramolecular recombination (Scheme 1).<sup>6</sup>

Inverse vulcanization is an efficient method to reuse sulfur; in fact, it allows the obtainment of high sulfur-containing polymeric materials with a sulfur content over 50 wt%. It has some advantages such as simplicity, scalability, and high atom efficiency and it is a solvent-free process.<sup>6</sup> However, the choice of crosslinker monomers is limited by the high temperature needed to cleave S–S bonds and low miscibility with  $S_8$ . Some authors have taken advantage of the ability of the structural rearrangement of polysulfides synthesized by inverse vulcanization for further treatment with a second low boiling crosslinker at a mild temperature.<sup>13,21,22</sup> Recently, another possible method to co-polymerize elemental sulfur, which is a catalytic pathway that requires temperatures lower than those for traditional inverse vulcanization, has been reported by Hasell and co-workers.<sup>13</sup> Metal salts, oxides and complexes effectively

<sup>a</sup>University of Milano Bicocca, Dep. Materials Science, via R. Cozzi, 55, 20125 Milano, Italy

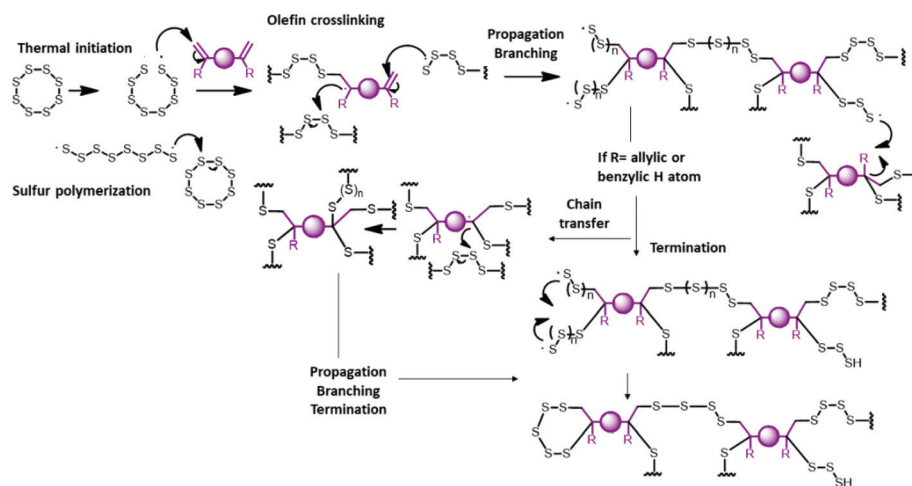
<sup>b</sup>CNR-SCITEC, Istituto di Scienze e Tecnologie Chimiche “Giulio Natta”, via A. Corti, 12, 20133 Milano, Italy. E-mail: incoronata.tritto@scitec.cnr.it

<sup>c</sup>INSTM, Via Giuseppe Giusti, 9, 50121 Firenze, Italy

† This work is dedicated to the memory of Dr Dino Romano Ferro, whose scientific originality, open mindedness, and kindness we have always heartily admired.

‡ Electronic supplementary information (ESI) available: Stability of poly(S-dipentene) and poly(S-dipentene-DAS) (Fig. S1). Preparation of objects and a film (Fig. S2 and S3). Metal chloride (aq) removal (Fig. S4 and S5). Elemental analysis (Table S1). Gas chromatography-mass spectrometry (GC-MS) of volatile compounds of poly(S-dipentene) (Fig. S6–S8). SEM analysis (Fig. S9). See DOI: <https://doi.org/10.1039/d2py00095d>





**Scheme 1** Inverse vulcanization mechanism.

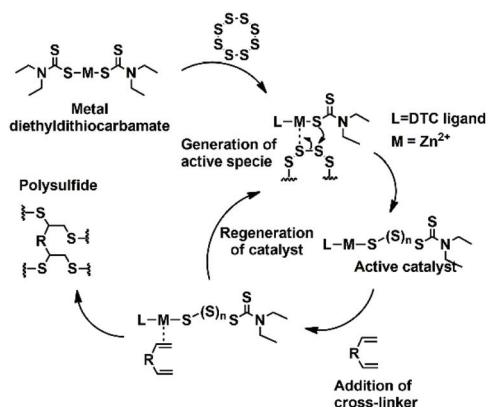
used as accelerators in conventional vulcanization were tested. In their study, they found that zinc diethyldithiocarbamate leads to rapid formation of solid polymers. They suggested that metals act like phase transfer agents to shuttle reactive sulfur into the diethyldithiocarbamate organic phase (Scheme 2), improving the miscibility between the organic crosslinker and molten sulfur phase, and making possible the reaction with monomers that are unreactive without catalysts, such as ethylene glycol dimethylacrylate, 1,3,5,7-tetravinyltetramethylcyclotetrasiloxane and glyoxal bis(diallylacetal).<sup>13</sup>

Motivated by the need to explore sustainable feedstocks to produce functional materials, some authors reported on limonene-based polymers, since every year over 70 thousand tons of limonene are isolated from orange peels in the citrus industry.<sup>3,23–26</sup> However, only a few references exist on limonene-based polysulfides.<sup>3,7,8,27–30</sup> Crockett and Hasell both developed wax-like polysulfides using *D*-limonene (50 wt%) from inverse vulcanization and catalytic inverse vulcanization, respectively. Crockett synthesized limonene polysulfide with a glass transition temperature ( $T_g$ ) equal to  $-21$  °C and mole-

cular weight ( $M_n$ ) under 800 Da, while Hasell used limonene to obtain polysulfide with higher  $T_g$  by performing the synthesis also in the presence of zinc diethyldithiocarbamate as the catalyst and obtaining  $T_g$  values of  $-3$  °C and  $5$  °C with 1 wt% and 5 wt% of the catalyst, respectively.<sup>13</sup>

Dipentene (Fig. 1) is a low-cost, bio-based mixture, produced from citrus oil on a large scale, and may represent a much more economical alternative to enantiomeric (*D* or *L*) limonene for the production of green polysulfides.<sup>7,8,11,31</sup> Dipentene is a mixture of monoterpene olefins and specifically of 3-carene, the most abundant component, racemic limonene and  $\alpha$  and  $\beta$ -pinene. It is widely used as a flavouring and fragrance agent and a green solvent (e.g. reaction media for the enzymatic synthesis of phosphatidylserine)<sup>32,33</sup> but to the best of our knowledge, it has never been used in inverse vulcanization reactions.

In this work, the synthesis of poly(*S*-dipentene) with a sulfur content greater than 50 wt% by catalytic inverse vulcanization in the presence of zinc-based accelerators was investigated. Inspired by Smith's work on new ter-polymers from sulfur and alkene monomers,<sup>34</sup> three bio-based dienes were used as crosslinkers in the post-polymerization of poly(*S*-dipentene), to obtain ter-polymers with depressed depolymerization reactions (Fig. 2). Moreover, the ter-polymers prepared were blended with commercial polystyrene and uniform, resist-



**Scheme 2** Mechanism of catalytic inverse vulcanization suggested by Hasell.<sup>13</sup>

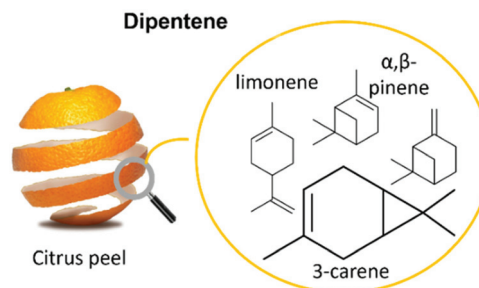


**Fig. 1** Dipentene mixture.



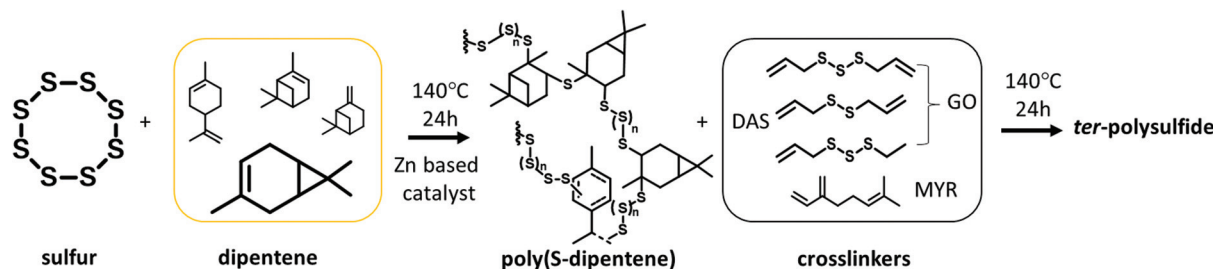


Fig. 2 Synthesis of dipentene-based polysulfides.

ant solids, completely soluble in THF and chloroform, were obtained. The obtained materials were moulded and a preliminary screening of the possible application in wastewater purification was performed.

## Experimental

### Materials

Sulfur powder (Alfa Aesar, 99.5%), dipentene (Sigma-Aldrich, technical grade, mixture of isomers), *R*-limonene (Sigma-Aldrich, 97%), myrcene (Sigma-Aldrich, technical grade), garlic oil blend (Sigma-Aldrich, food grade), zinc 2-mercaptobenzothiazole (TCI, >98%), zinc diethyldithiocarbamate (Sigma-Aldrich, 97%), zinc *O,O,O',O'*-tetrabutyl-bis(phosphorodithioate) (Alfa Chemistry, 98%), zinc isopropylxanthate (Alfa Chemistry), Polystyrene Edistir 2380© and NaCl (Sigma-Aldrich, ReagentPlus, ≥99%) were commercially available and used as received.

### General polymerization of S<sub>8</sub> and dipentene on a 2.5 g scale

In a 22 mL glass vial, equipped with a magnetic stir bar and closed with a rubber septum pierced with a needle to degas the system, 1.5 g of elemental sulfur powder, 1 g of dipentene and 25 mg of the accelerator were added. The vial was heated without stirring in a metal heating block set to 140 °C until sulfur was melted. After 10 minutes, the needle was removed, and stirring was performed at 335 rpm. The system was degassed for 1 or 2 s five times each for 30 min and then it was degassed continuously for 3 hours. The reaction was left in the heating blocks for 24 hours and after it was cooled to room temperature. A typical poly(S-dipentene) contains 65.77 wt% of sulfur (Table S1†).

### General post-polymerization of poly(S-dipentene) on a 2.5 g scale

To the polysulfide prepared according to the procedure described above, contained in a 22 mL glass vial equipped with a magnetic stir bar, 10 wt% of the second crosslinker with respect to the polysulfide weight was added. The vial was closed with a rubber septum pierced with a needle and was heated under stirring at 335 rpm in a metal heating block set. The reaction was left in the heating blocks for 24 hours and after it was cooled to room temperature. The polysulfides were

heated to 80 °C and volatile compounds were extracted by vacuum distillation. The materials were not further purified. The yields, measured by comparing the weight before and after vacuum distillation, were almost quantitative (97 wt%).

### General polymerization of poly(S-dipentene) and DAS on a 110 g scale

Sulfur (60 g) and ZBDP (1.53 g) were added to a 250 mL three neck flask equipped with a mechanical stirrer. The flask was placed in an oil bath heated to 140 °C and only when the sulfur was completely melted, the agitation was started. After this, dipentene (40 g) was added using a syringe and left for 2.5 h, resulting in a two-phase mixture. The system was degassed after 15 minutes from dipentene addition and after each 30 min for 3 h. The reaction was left for 5 hours and then it was cooled to room temperature. Later, poly(S-dipentene) was re-heated to 140 °C under stirring and diallyl sulfide (10 g) was added. The reaction was left for 5 hours and then it was cooled to room temperature. Poly(S-dipentene-DAS) was heated to 80 °C and volatile compounds were extracted by vacuum distillation. The yields, measured by comparing the weight before and after vacuum distillation, were almost quantitative (97 wt%). A typical poly(S-dipentene-DAS) contains 63.62 wt% of sulfur (Table S1†).

### Polystyrene-polysulfide blend preparation

The same amounts of poly(S-dipentene-DAS) and Edistir 2380© were solubilized in chloroform under stirring; then, 70 wt% of NaCl with respect to the polymeric component was added. Afterwards, chloroform was removed and the resultant salt templated polymer was ground and mixed in distilled water under stirring for four days to solubilize NaCl. Later, the polymer was washed with methanol and dried in an oven overnight at 40 °C, under reduced pressure.

### Preparation of samples for residual metal content determination

Aqueous solutions of FeCl<sub>3</sub>, CuCl<sub>2</sub>, NiCl<sub>2</sub>, CrCl<sub>2</sub> and CoCl<sub>2</sub> at a concentration of 100 ppm were prepared and equilibrated for 24 h. Inside a closed vial, 1 g of the ground material was soaked in 20 mL of the solution containing a given type of salt. After 2 or 24 hours of incubation under static conditions (without mixing), an aliquot of the supernatant solution was



taken and the residual metal content was measured by ICP-OES.

### Polymer characterization

$^1\text{H-NMR}$  samples were obtained by dissolution of 15 mg of the sample in  $\text{CDCl}_3$  in a 5 mm tube.  $^1\text{H-NMR}$  spectra were acquired on a Bruker Avance DRX 600 spectrometer operating at 600 MHz at room temperature.  $\text{CDCl}_3$  (standardization of chemical shifts of TMS at 7.24 ppm) was used as the internal chemical shift reference. The applied conditions were the following: 5 mm probe,  $90^\circ$  pulse angle, 32 K data points, acquisition time of 2.20 s, relaxation delay of 2 s, and 64 transients.

Gel permeation chromatography (GPC) analyses were performed on a Waters GPCV2000 system, using THF with 0.05 wt% of BHT as the antioxidant as the mobile phase, at  $35^\circ\text{C}$  with a  $0.6\text{ mL min}^{-1}$  flow. The sample concentration was set at  $2\text{ mg mL}^{-1}$  and the injection volume at  $150\ \mu\text{L}$ . The calibration of the curves was performed using polystyrene standards in the 162–800 000 Da range.

Differential scanning calorimetry (DSC) measurements were performed on a PerkinElmer DSC 8000 instrument. The scans were carried out from  $-20$  to  $120^\circ\text{C}$  under a nitrogen atmosphere using heating and cooling rates of  $20^\circ\text{C min}^{-1}$ .

Thermogravimetric tests were performed using a PerkinElmer TGA 7 at  $20^\circ\text{C min}^{-1}$ . Each sample was investigated in the thermal range from 50 to  $500^\circ\text{C}$  under nitrogen.

Infrared spectra (ATR-IR) were recorded on a PerkinElmer Spectrum Two spectrometer at room temperature directly on the solid material.

Scanning electron microscopy (SEM) images were obtained using an SEM-EDX TM1000 Hitachi at the University of Milan. The samples were coated with gold nanoparticles before performing SEM imaging.

## Results and discussion

The catalytic inverse vulcanization of dipentene, in the presence of four different chemical classes of zinc-based accelerators (Table 1), commonly used in traditional rubber vulcanization, was investigated. Of all of them, ZMBT, ZDTC, ZBDP and ZIX, only ZDTC was first reported by Hasell in inverse vulcanization, while the others were unexplored until now.<sup>35</sup>

In this work, an excess amount of sulfur with respect to dipentene to maximize the content of sulfur in the final material was used, while in most studies, over 50 wt% of limonene was used to prevent the “sulfur bloom” which results in inhomogeneity, and to stabilize limonene polysulfide.<sup>7</sup>

Poly(S-dipentene) was obtained by heating six parts of sulfur, four parts of dipentene and 1 wt% of the catalyst at  $140^\circ\text{C}$  for 24 h under vigorous stirring, starting from experimental conditions used by Hassel for the synthesis of limonene polysulfide in the presence of ZDTC.<sup>13</sup> Catalysts reduced the mixing time between sulfur and dipentene. Indeed, the mixing time between molten sulfur and dipentene reduced from two hours, in the absence of the accelerator, to 30 minutes when ZMBT or ZBDP were used and to 50 minutes in the presence of ZDTC and ZIX. Without any catalyst, a yellow solid product was obtained in a few hours ( $<12\text{ h}$ ), indicating a depolymerization reaction and the formation of  $\text{S}_8$  crystals (Table 2).

Interestingly, when polysulfides were obtained in the presence of an accelerator, they appeared as wax-like dark brown materials. The stability of polysulfides depends on the accelerator used. Polysulfides obtained with ZMBT and ZDTC become yellow after 24 h, whereas those produced with ZBDP and ZIX become inhomogeneous after 36 h (Table 2 and Fig. S1†). Thus, accelerators are able to reduce the mixing time between sulfur and dipentene and minimize the loss of mass by evaporation of dipentene during polysulfide production, probably for their ability to transfer reactive sulfur into the organic phase, according to the mechanism suggested by Hasell.<sup>13</sup>

**Table 2** Catalytic inverse vulcanization of dipentene<sup>a</sup>

Entry	Accelerator	Mixing time (min)	Depolymerization time <sup>b</sup> (h)
1	—	120	Before 12
2	ZMBT	30	After 24
3	ZDTC	50	After 24
4	ZBDP	30	After 36
5	ZIX	50	After 36

<sup>a</sup> Dipentene = 1 g,  $\text{S}_8/\text{dipentene}$  = 60/40 wt%, accelerator = 25 mg,  $T = 140^\circ\text{C}$ ,  $t = 24\text{ h}$ . <sup>b</sup> Time for depolymerization and “sulfur bloom” formation.

**Table 1** Different accelerators used in the inverse vulcanization of the S-dipentene co-polymer

Name	Class	Acronym	Formula
Zinc 2-mercaptobenzothiazole	Thiazoles	ZMBT	
Zinc diethyldithiocarbamate	Thiocarbamates	ZDTC	
Zinc O,O',O'-tetrabutyl-bis(phosphorodithioate)	Thiophosphate	ZBDP	
Zinc isopropylxanthate	Xanthates	ZIX	



In order to improve the poly(S-dipentene) stability, a second bio-based crosslinker was added. Three natural dienes (Fig. 3) were tested in the post-polymerization of polysulfide: myrcene (MYR), a natural terpene obtained from the essential oil of different plants like thyme; garlic oil (GO), composed of diallyl trisulfide, diallyl disulfide and allyl methyl trisulfide; and diallyl disulfide (DAS), which is present also in onions and is responsible for the typical odor.<sup>11,36</sup>

The crosslinker (10 wt%) was added to poly(S-dipentene) previously synthesized with ZBDP and ZIX (entries 4 and 5 in Table 2) as reported in Table 3. We decided not to use quantities exceeding 10 wt% of a further crosslinker to maintain the sulfur percentage in the final material close to 50 wt%, providing a stable sulfur-rich polymer with a final sulfur content of 54 wt%. Dark brown soft materials were obtained and no depolymerization phenomena were observed (Fig. S1†). The thermal properties of the synthesized polysulfides will be described in the following section "Thermal characterization".

All the polymers obtained are fully soluble in chloroform and tetrahydrofuran. The solubility of polysulfides has made possible <sup>1</sup>H-NMR and SEC characterization. In Fig. 4, the

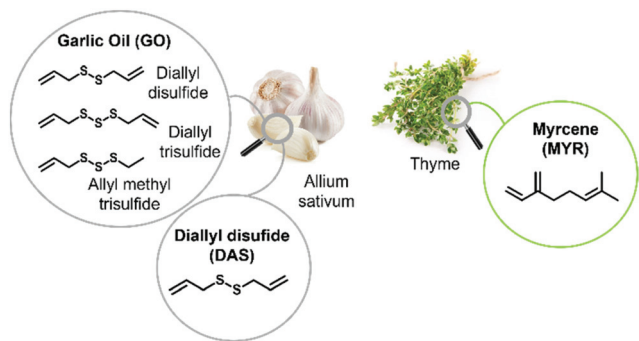


Fig. 3 Crosslinkers used: (a) garlic oil composed of diallyl disulfide, diallyl trisulfide and allyl methyl trisulfide, (b) diallyl disulfide and (c) myrcene.

Table 3 Co- and ter-polymer composition and thermal characterization<sup>a</sup>

Entry	Accelerator <sup>a</sup>	Additional crosslinker <sup>b</sup>	<i>T<sub>g</sub></i> (°C)
6	ZBDP	—	1
7		MYR	2
8		GO	1
9		DAS	4
10	ZIX	—	-1
11		MYR	2
12		GO	0
13		DAS	-1
1	—	—	-2
14		MYR	3
15		GO	0
16		DAS	-1

<sup>a</sup> Dipentene = 1 g, S<sub>8</sub>/dipentene = 60/40 wt%, accelerator = 25 mg, *T* = 140 °C, *t* = 24 h. <sup>b</sup> Additional crosslinker = 250 mg, *T* = 140 °C, *t* = 24 h.

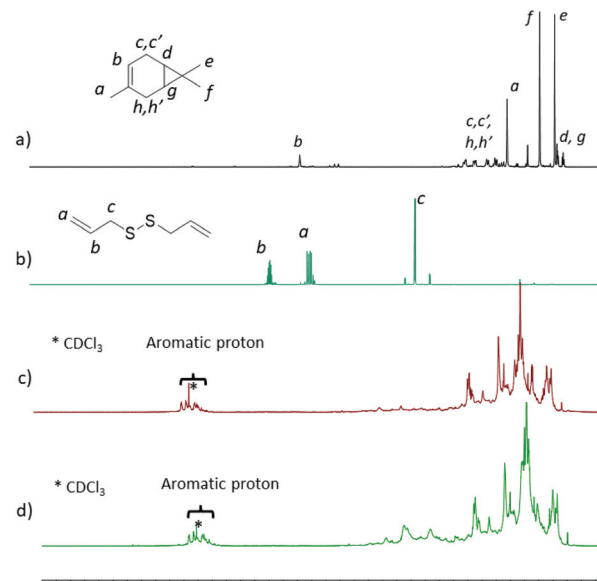


Fig. 4 <sup>1</sup>H-NMR spectra of (a) dipentene, (b) diallyl disulfide (DAS), (c) poly(S-dipentene), and (d) poly(S-dipentene-DAS).

<sup>1</sup>H-NMR spectra of poly(S-dipentene) (entry 4) (Fig. 4c) and poly(S-dipentene-diallyl disulfide) (entry 9) (Fig. 4d) are compared with those of dipentene (Fig. 4a) and DAS (Fig. 4b), taken as references. Fig. 4a shows the resonances belonging to the 3-carene structure (signals of methine protons from 0.64 to 0.74 ppm, signals of methyl protons from 0.79 to 1.62 ppm, signals of methylene protons from 1.80 to 2.40 ppm and signal of a vinylic proton at 5.26 ppm). The comparison between Fig. 4a and c revealed the absence of vinyl proton signals and the broadening of peaks between 0.64 to 2.40 ppm due to polymerization.<sup>37</sup> The resonances in Fig. 4c between 2.5 and 4.0 ppm were assigned to methine and methylene protons –S–CH<sub>x</sub>–.<sup>22</sup> The addition of a ter-monomer, DAS (Fig. 4d), and its subsequent vulcanization increased the intensity of signals related to –S–CH<sub>x</sub>– bonds in the ter-polymer. The presence of resonances assigned to aromatic protons between 7.0 and 7.5 ppm could be ascribed to the dehydrogenation of the monomer, already observed for inverse vulcanization of limonene.<sup>8,37</sup>

The chemical nature of poly(S-dipentene) and poly(S-dipentene-DAS) was further investigated by ATR-IR (Fig. 5). The complete absence of absorption peaks related to double bonds which, usually, appear at 3100 cm<sup>-1</sup> (–C=C–H stretching), 1660 cm<sup>-1</sup> (–C=C– bending), 990 cm<sup>-1</sup> and 910 cm<sup>-1</sup> (–C=C–H bending) was noted. In addition, no peaks were detected between 2550 and 2620 cm<sup>-1</sup>, attributed to the thiol group.<sup>7</sup> The presence of bands below 3000 cm<sup>-1</sup> and between 1450 cm<sup>-1</sup> and 1350 cm<sup>-1</sup> were linked to the –C–H stretching and bending of the alkyl group.<sup>11</sup> Moreover, the stretching of –C–S– and –S–S– bonds was noticed below 700 cm<sup>-1</sup> (Fig. 5).<sup>38</sup>

SEC characterization indicated the formation of low molecular weight materials (*M<sub>n</sub>* < 1000 Da).



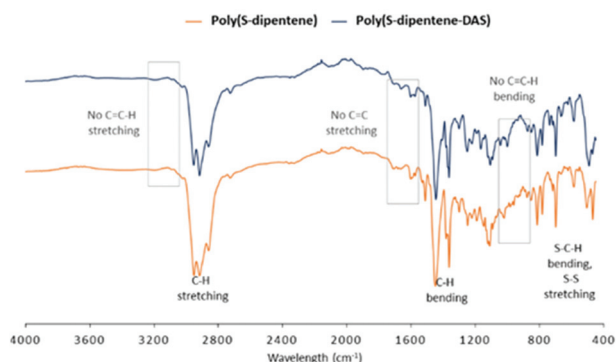


Fig. 5 ATR-IR spectra of poly(S-dipentene) (blue line) and poly(S-dipentene-DAS) (orange line).

### Thermal characterization

Thermal gravimetric analysis (TGA) was performed for all the polysulfides showing a midpoint decomposition temperature around 250 °C. Differential scanning calorimetry (DSC) of poly(S-dipentene) with ZBDP and ZIX revealed  $T_g$  values of 1 °C and -1 °C, respectively, and no crystallization of sulfur was detected. The addition of 10 wt% of a ter-monomer slightly changes the  $T_g$  values (Fig. 6 and Table 3). The glass transition temperature of poly(S-dipentene-MIR) was found to be 2 °C with both ZBDP and ZIX. Different  $T_g$  values were observed for poly(S-dipentene-DAS) depending on the catalyst used during its synthesis: 4 °C with ZBDP and -1 °C with ZIX. The  $T_g$  values for poly(S-dipentene-GO) prepared with ZBDP and ZIX were similar, 1 °C and 0 °C, respectively. Overall, ZBDP led to an increase of the  $T_g$  values of a few degrees for all polysulfides except for poly(S-dipentene-MIR). However, all poly(S-dipentene-MIR) and poly(S-dipentene-DAS) prepared with ZBDP were stable, having  $T_g$  values higher than poly(S-dipentene).

We carried out the synthesis of several poly(S-limonene)s with ZDTC and ZBDP at two different ratios, 60/40 and 50/50 wt%, in order to compare their properties with those of poly(S-limonene)s found in the literature and with poly(S-

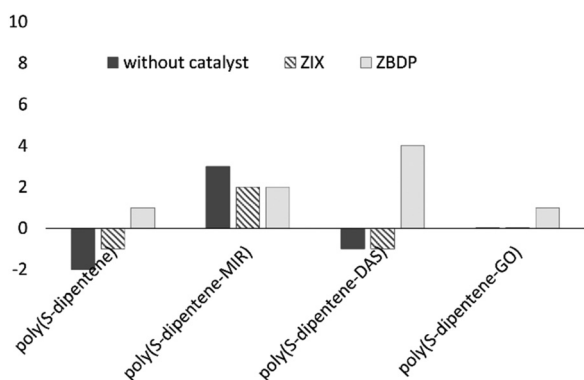


Fig. 6 Glass transition temperatures of co- and ter-polymers of Table 3: poly(S-dipentene) with sulfur content = 60 wt%, poly(S-dipentene-crosslinker) with sulfur content = 54 wt%.

dipentene)s. ZDTC and ZBDP were chosen since ZDTC was the accelerator used by Hasell and ZBDP was the highest performing catalyst for poly(S-dipentene)s. Poly(S-limonene)s prepared under our conditions were soft solids and interestingly, they exhibited a higher glass transition temperature than those reported in the literature for poly(S-limonene)s prepared with 50/50 wt% (entry 19 vs. entries 17 and 18, conducted in the absence of the accelerator, and entry 21 vs. entry 20 with ZDTC in Table 4).<sup>8,13</sup> Indeed, the addition of the accelerator had a marked effect on  $T_g$  values which reached 7 °C in the absence of the accelerator and 17 °C with 1 wt% of ZDTC.

ZBDP, which provided the most stable poly(S-dipentene), led to poly(S-limonene) with  $T_g$  lower than that obtained with ZDTC. Overall, under our conditions, limonene polysulfide presented  $T_g$  higher than poly(S-dipentene), which probably depends on the higher structural order of poly(S-limonene) and no depolymerization phenomena were observed.

### Polystyrene-polysulfide blend

In order to prepare processable ter-polysulfides and to give them shape persistence for possible applications,<sup>39-41</sup> polystyrene-polysulfide blends were prepared. Poly(S-dipentene-DAS) (entry 9) was selected for the higher  $T_g$  detected. Polystyrene was chosen for its high solubility in chloroform and tetrahydrofuran, similar to the polysulfide, and for its relatively low temperature of extrusion and moulding compatible with polysulfide degradation temperature. The polystyrene blend was prepared by simultaneous solubilization and mixing of poly(S-dipentene-DAS) and polystyrene (50/50 wt%) in chloroform and a salt templating technique; the resulting material was successively dried to remove the solvent. The blend appeared as a dark orange, uniform, smooth, and resistant solid which maintains its shape at room temperature. It shows  $T_g$  equal to 44 °C and is completely soluble in THF and chloroform. The blend was ground and then melted and pressed at 120 °C to obtain a thin layer of the material that exhibited flexibility (Fig. 7). The thermoplastic character of the blend makes it possible to produce a series of objects and to

Table 4 Glass transition temperature ( $T_g$ ) related to different polysulfides<sup>a,b</sup>

Entry	Polysulfide comonomer	Catalyst	S <sub>g</sub> /comonomer	$T_g$ (°C)
1	Dipentene <sup>a</sup>	—	60/40	-2
4	Dipentene <sup>a</sup>	ZBDP (1%)	60/40	1
17	Limonene <sup>c</sup>	—	50/50	-21
18	Limonene <sup>d</sup>	—	50/50	0
19	Limonene <sup>b</sup>	—	50/50	7
20	Limonene <sup>d</sup>	ZDTC (1%)	50/50	-3
21	Limonene <sup>b</sup>	ZDTC (1%)	50/50	17
22	Limonene <sup>b</sup>	ZBDP (1%)	50/50	9
23	Limonene <sup>a</sup>	—	60/40	10
24	Limonene <sup>a</sup>	ZBDP (1%)	60/40	7

<sup>a</sup> Comonomer (dipentene or limonene) = 1 g, accelerator = 25 mg,  $T = 140$  °C,  $t = 24$  h. <sup>b</sup> Limonene = 1.5 g, accelerator = 25 mg,  $T = 140$  °C,  $t = 24$  h. <sup>c</sup> Poly(S-limonene) synthesized by Crockett.<sup>8</sup> <sup>d</sup> Poly(S-limonene) synthesized by Hasell.<sup>13</sup>



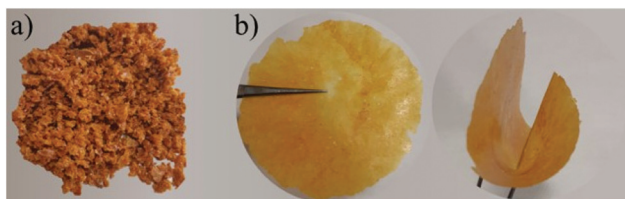


Fig. 7 Polystyrene-ter-polysulfide: (a) ground and (b) pressed.

change their shape several times. This ability gives a promising perspective for the application of this material.

The scanning electron microscopy (SEM) images of the porous and hot pressed polystyrene-ter-polysulfide blend were obtained and are shown in Fig. 8 and Fig. S9.† It is evident from Fig. 8a that the salt templating technique produced inhomogeneous and irregular macropores, while the SEM image of the hot pressed film shows a quite smooth surface, without phase separations and pores (Fig. 8b).

Polysulfides can find application in environmental remediation.<sup>7–10,42</sup> Thus, their use can become helpful against wastewater contamination, which is a growing concern in industrialized and developing countries. Pollution from copper, nickel, cobalt and chromium is of great concern to human health because these metals are highly toxic, already, at low doses.<sup>43,44</sup> Furthermore, also the iron content in potable water and wastewater is regulated because, in particular, ferric iron

produces plumbing fixture discolouration, leads to the growth of bacteria and gives an odour and taste to drinking water.<sup>9</sup>

Reports on the polysulfide capture of mercury, palladium and iron are present in the literature; however, there is a lack of publications on copper ( $\text{Cu}^{2+}$ ), nickel ( $\text{Ni}^{2+}$ ), chromium ( $\text{Cr}^{2+}$ ) and cobalt ( $\text{Co}^{2+}$ ) capture. For this reason, a preliminary screening of the ability of the polystyrene-ter-polysulfide blend to bind and remove iron ( $\text{Fe}^{3+}$ ), copper ( $\text{Cu}^{2+}$ ), nickel ( $\text{Ni}^{2+}$ ), chromium ( $\text{Cr}^{2+}$ ) and cobalt ( $\text{Co}^{2+}$ ) from water was performed.

It was found that the polysulfide blend selectively removes ferric ions, leading to a reduction in their concentration of 33% and 83% after 2 h and 24 h, respectively. However, no changes in the concentrations of  $\text{Cu}^{2+}$ ,  $\text{Ni}^{2+}$ ,  $\text{Cr}^{2+}$  and  $\text{Co}^{2+}$  were observed after 24 h of contact between the metal solutions and the polysulfide blend with the methodology used. Moreover, no colour variation or deposit was identified. A more detailed study is underway to understand this behaviour.

## Conclusions

For the first time, an investigation of the inverse vulcanization of dipentene for the production of polysulfides with a sulfur content greater than 50 wt% in the presence of zinc base accelerators was performed. Accelerators reduced the mixing time between dipentene and melted sulfur probably acting as phase transfer agents. In poly(S-dipentene)s, depolymerization phenomena were observed due to a high percentage of sulfur (60 wt%) even if the presence of accelerators delays its occurrence. Depolymerization phenomena were suppressed by adding 10 wt% of MYR, GO or DAS to poly(S-dipentene). The ter-polysulfides produced are soft solids with  $T_g$  values between  $-1$  and  $4$  °C.

Moreover, polystyrene-polysulfide blends were prepared to make our ter-polysulfides processable and to make them available for possible applications where shape persistence is a fundamental requirement. Moreover, it was found that the polystyrene-poly(S-dipentene-DAS) blend was able to bind and remove ferric ions from aqueous solutions. This material showed shape persistence and can be moulded to produce iron binding objects such as filter disposables, which could be a viable alternative for water remediation, especially in developing countries, where conventional methods for water treatments such as membrane filtration, activated carbon absorption and electrocoagulation, often, are not feasible.

In conclusion, stable ter-polysulfides with low cost, bio-based dipentene mixture and MYR and DAS, endowed with  $T_g$  values lower but comparable to those of poly(S-limonene) were achieved and they may represent a much more economical alternative to green polysulfides produced with enantiomeric (D) limonene.

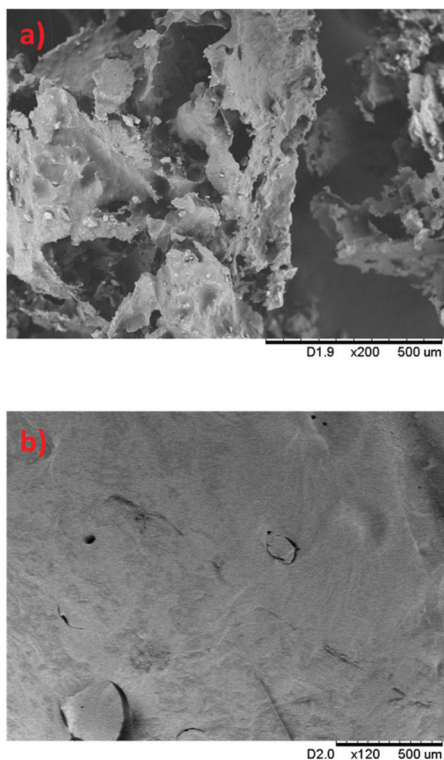


Fig. 8 SEM images of the metalated polystyrene-poly(S-dipentene-DAS) blend with 50 wt% of polystyrene after salt templating (a) and after hot press (b).

## Conflicts of interest

There are no conflicts to declare.



## Notes and references

- 1 Statistical Review of World Energy 2020 69<sup>th</sup> edition, <https://www.bp.com/en/global/corporate/energy-economics/statistical-review-of-world-energy.html>, (accessed 9-02-2021, 2021).
- 2 V. Chandra Srivastava, *RSC Adv.*, 2012, **2**, 759–783.
- 3 M. J. H. Worthington, R. L. Kucera and J. M. Chalker, *Green Chem.*, 2017, **19**, 2748–2761.
- 4 D. A. Boyd, *Angew. Chem., Int. Ed.*, 2016, **55**, 15486–15502.
- 5 J. J. Griebel, R. S. Glass, K. Char and J. Pyun, *Prog. Polym. Sci.*, 2016, **58**, 90–125.
- 6 W. Chung, J. Griebel, E. Kim, H. Yoon, A. Simmonds, H. Ji, P. Dirlam, R. Glass, J. J. Wie, N. Nguyen, B. Guralnick, J. Park, A. Somogyi, P. Theato, M. Mackay, Y. E. Sung, K. Char and J. Pyun, *Nat. Chem.*, 2013, **5**, 518–524.
- 7 D. J. Parker, H. A. Jones, S. Petcher, L. Cervini, J. M. Griffin, R. Akhtar and T. Hasell, *J. Mater. Chem.*, 2017, **5**, 11682–11692.
- 8 M. P. Crockett, A. M. Evans, M. J. H. Worthington, I. S. Albuquerque, A. D. Slattery, C. T. Gibson, J. A. Campbell, D. A. Lewis, G. J. L. Bernardes and J. M. Chalker, *Angew. Chem., Int. Ed.*, 2016, **55**, 1714–1718.
- 9 N. A. Lundquist, M. J. H. Worthington, N. Adamson, C. T. Gibson, M. R. Johnston, A. V. Ellis and J. M. Chalker, *RSC Adv.*, 2018, **8**, 1232–1236.
- 10 M. J. H. Worthington, C. J. Shearer, L. J. Esdaile, J. A. Campbell, C. T. Gibson, S. K. Legg, Y. Yin, N. A. Lundquist, J. R. Gascooke, I. S. Albuquerque, J. G. Shapter, G. G. Andersson, D. A. Lewis, G. J. L. Bernardes and J. M. Chalker, *Adv. Sustainable Syst.*, 2018, **2**, 1800024–1800031.
- 11 I. Gomez, O. Leonet, J. A. Blazquez and D. Mecerreyes, *ChemSusChem*, 2016, **9**, 3419–3425.
- 12 J. J. Griebel, S. Namnabat, E. T. Kim, R. Himmelhuber, D. H. Moronta, W. J. Chung, A. G. Simmonds, K.-J. Kim, J. van der Laan, N. A. Nguyen, E. L. Dereniak, M. E. Mackay, K. Char, R. S. Glass, R. A. Norwood and J. Pyun, *Adv. Mater.*, 2014, **26**, 3014–3018.
- 13 X. Wu, J. A. Smith, S. Petcher, B. Zhang, D. J. Parker, J. M. Griffin and T. Hasell, *Nat. Commun.*, 2019, **10**, 647, DOI: [10.1038/s41467-019-08430-8](https://doi.org/10.1038/s41467-019-08430-8).
- 14 S. Silvano, C. F. Carrozza, A. R. de Angelis, I. Tritto, L. Boggioni and S. Losio, *Macromolecules*, 2020, **53**, 8837–8846.
- 15 C. Tavella, P. Lova, M. Marsotto, G. Luciano, M. Patrini, P. Stagnaro and D. Comoretto, *Crystals*, 2020, **10**, 154, DOI: [10.3390/cryst10030154](https://doi.org/10.3390/cryst10030154).
- 16 K. S. Kang, A. Phan, C. Olikagu, T. Lee, D. A. Loy, M. Kwon, H.-J. Paik, S. J. Hong, J. Bang, W. O. Parker Jr., M. Sciarra, A. R. de Angelis and J. Pyun, *Angew. Chem., Int. Ed.*, 2021, **60**, 22900–22907.
- 17 T. Lee, P. T. Dirlam, J. T. Njardarson, R. S. Glass and J. Pyun, *J. Am. Chem. Soc.*, 2022, **144**, 5–22.
- 18 Y. Zhang, R. S. Glass, K. Char and J. Pyun, *Polym. Chem.*, 2019, **10**, 4078–4105.
- 19 J. M. Chalker, M. J. H. Worthington, N. A. Lundquist and L. J. Esdaile, *Top. Curr. Chem.*, 2019, **377**, 16, DOI: [10.1007/s41061-019-0242-7](https://doi.org/10.1007/s41061-019-0242-7).
- 20 J. Chalker, M. Mann, M. Worthington and L. Esdaile, *Org. Mater.*, 2021, **3**, 362–373.
- 21 C. R. Westerman and C. L. Jenkins, *Macromolecules*, 2018, **51**, 7233–7238.
- 22 Y. Zhang, K. M. Konopka, R. S. Glass, K. Char and J. Pyun, *Polym. Chem.*, 2017, **8**, 5167–5173.
- 23 S. Neumann, P. Hu, F. Bretschneider, H. Schmalz and A. Greiner, *Macromol. Mater. Eng.*, 2021, **306**, 2100090–2100102.
- 24 E. G. Andriotis, A. E. Koumbis and D. S. Achilias, *Polym. Bull.*, 2021, **78**, 4609–4628.
- 25 M. P. Arrieta, J. Lopez, S. Ferrandiz and M. A. Peltzer, *Polym. Test.*, 2013, **32**, 760–768.
- 26 C. A. Brito and A. C. Silvino, *Rev. Virtual Quim.*, 2021, **13**, 1017–1041.
- 27 J. M. Chalker, M. P. Crockett, A. M. Evans and M. Worthington, US10590012, 2015.
- 28 T. Hasell, D. J. Parker, H. A. Jones, T. McAllister and S. M. Howdle, *Chem. Commun.*, 2016, **52**, 5383–5386.
- 29 F. Wu, S. Chen, V. Srot, Y. Huang, S. K. Sinha, P. A. van Aken, J. Maier and Y. Yu, *Adv. Mater.*, 2018, **30**, 1706643–1706651.
- 30 M. Worthington, I. Y. Muhti, M. Mann, Z. Jia, A. Miller and J. Chalker, *ChemRxiv*, 2022, DOI: [10.26434/chemrxiv-2022-ss450](https://doi.org/10.26434/chemrxiv-2022-ss450).
- 31 Differences in costs between dipentene and enantiomeric limonene: dipentene costs range from 40 to 60 euros per kg, while enantiomeric limonene costs range from 70 to 80 euros per kg (from Sigma-Aldrich catalogue).
- 32 E. Jongedijk, K. Cankar, J. Ranzijn, A. Krol, H. Bouwmeester and J. Beekwilder, *Yeast*, 2014, **32**, 159–171.
- 33 Y. H. Bi, Z. Q. Duan, W. Y. Du and Z. Y. Wang, *Biotechnol. Lett.*, 2014, **37**, 115–119.
- 34 J. A. Smith, S. J. Green, S. Petcher, D. J. Parker, B. Zhang, M. J. H. Worthington, X. Wu, C. A. Kelly, T. Baker, C. T. Gibson, J. A. Campbell, D. A. Lewis, M. J. Jenkins, H. Willcock, J. M. Chalker and T. Hasell, *Chem. – Eur. J.*, 2019, **25**, 10433–10440.
- 35 Polymer properties database, <https://polymerdatabase.com/polymer%20chemistry/Vulcanization%20Accelerators.html>, (accessed 10/12/20, 2020).
- 36 P. Satyal, J. D. Craft, N. S. Dosoky and W. N. Setzer, *Foods*, 2017, **6**, 63–73.
- 37 D. J. Parker, S. T. Chong and T. Hasell, *RSC Adv.*, 2018, **8**, 27892–27899.
- 38 C. N. R. Rao, R. Venkataraghavan and T. R. Kasturi, *Can. J. Chem.*, 1964, **42**, 36–42.
- 39 N. A. Lundquist, A. D. Tikoalu, M. J. H. Worthington, R. Shapter, S. J. Tonkin, F. Stojcevski, M. Mann, C. T. Gibson, J. R. Gascooke, A. Karton, L. C. Henderson, L. J. Esdaile and J. M. Chalker, *Chem. – Eur. J.*, 2020, **26**, 10035–10044.



- 40 I. Bu Najmah, N. A. Lundquist, M. K. Stanfield, F. Stojcevski, J. A. Campbell, L. J. Esdaile, C. T. Gibson, D. A. Lewis, L. C. Henderson, T. Hasell and J. M. Chalker, *ChemSusChem*, 2021, **14**, 2352–2359.
- 41 M. W. Thielke, L. A. Bultema, D. D. Brauer, B. Richter, M. Fischer and P. Theato, *Polymers*, 2016, **8**, 266–275.
- 42 X. Jiang, *Sulfur Chemistry*, Springer, Switzerland, 2019.
- 43 M. Thomas, B. Bialecka and D. Zdebik, *Arch. Environ. Prot.*, 2018, **44**, 33–47.
- 44 L. Joseph, B. M. Jun, J. R. V. Flora, C. M. Park and Y. Yoon, *Chemosphere*, 2019, **229**, 142–159.

